

A Search for Evaporation Residues in the $^{254}\text{Es}(^{16}\text{O},4n)107$ Reaction

M. Schädel, W. Brüche, E. Jäger, K. Sümmerer
 GSI Darmstadt

E. K. Hulet, J. F. Wild, R. W. Lougheed, R. J. Dougan, K. J. Moody
 LLNL Livermore, CA

Recent microscopic mass calculations by Möller et al.¹ have indicated that there is a small region of deformed nuclei around neutron number $N=162$ that is especially stable against spontaneous fission with barrier heights up to a maximum of about 7 MeV. From a very recent compilation² of experimental and calculated data a barrier height of about 5 MeV can be extrapolated for $Z=107$ nuclides in the $N=160$ region. Earlier calculations performed by Cwiok et al.^{3,4} obtained even slightly higher barriers. These rather high barriers, together with the experimentally observed α -decay of isotopes of elements 106 and heavier⁵, lend new hope that nuclides in this neutron-rich region may be synthesized by complete-fusion heavy-ion reactions. All reactions with compound nuclei in the $Z=107$, $N=160$ region require actinide targets and lead to a minimum excitation energy of about 40 MeV at the Coulomb barrier. Nuclides in this region are no more accessible in so called 'cold-fusion' reactions⁵. The isotope ^{254}Es as a target has the advantages that the most neutron-rich compound nuclei can be formed, and that one can hope for the lowest possible fusion hindrance because of the highest possible asymmetry in the entrance channel. While earlier parametrizations⁵ have strongly favoured such asymmetric combinations one does not find such a high advantage in more recent works².

Calculations indicate that with a fission barrier of only 3.5 MeV the cross section for the formation of $^{266}107$ from the $^{254}\text{Es}(^{16}\text{O},4n)$ reaction at 94 MeV is about 1 nb increasing to about 60 nb for a 5.5 MeV fission barrier. Table 1 shows the half-lives and decay predictions for isotopes of element 107 in this region.

Table 1: Half-life and decay predictions for element 107 isotopes

Nuclide	$t_{1/2}(\alpha)$	$t_{1/2}(\text{EC})$	decay of EC daughter
107-265	4s	1 min	SF(or EC or alpha with $t_{1/2}=5$ min)
107-266	2 min	2 min	SF-short $t_{1/2}$
107-267	5 min	2 min	SF(or EC, $t_{1/2}=10$ min)

In a series of experiments we have irradiated a $49 \mu\text{g}/\text{cm}^2$ ^{254}Es target (81% isotopic purity; electrodeposited onto a $4.5 \text{ mg}/\text{cm}^2$ Mo substrate) with beams of typically one particle- μAh of ^{16}O from the 88-inch cyclotron at the Lawrence Berkeley Laboratory. Reaction products, recoiling from the Es target, were stopped in a KCl-loaded He gas and were rapidly transported (≤ 0.5 s) to our on-line gas-phase chemistry apparatus OLGA. After an on-line chemical separation⁶ of actinide elements in the gas phase the transactinides were deposited onto thin tantalum coated $0.67 \text{ mg}/\text{cm}^2$ Ni foils, and were rotated

stepwise to seven sequential counting stations for α - and sf-measurements. Stepping (collection) times of 5s and 30s were chosen, respectively.

In two series of experiments with 93 MeV and 96 MeV of ^{16}O ions (energy in the target) we accumulated total doses of 1×10^{17} and 5×10^{16} particles, respectively. The energies chosen correspond to the calculated cross section maxima of the excitation function for the production of $^{266}107$ as obtained from two different evaporation codes.

A sum spectrum from 13 runs, all with a stepping time of 30s, and a total dose of 9.7×10^{16} particles (93 MeV - ^{16}O) accumulated over a time period of 21.4 hours is shown in Fig. 1. All peaks below an alpha energy of 7.5 MeV can be assigned to small amounts of Fm and Md isotopes not removed by the gas phase chemistry (decontamination factor of $\geq 10^3$). A total of 13 events were observed between 8.0 and 9.0 MeV. The assignment of these events to (1) non actinide contaminants like ^{212}Po , (2) known isotopes of heavy elements like Lr-257,258 or 105-261,262, or (3) a new isotope has to await a further and detailed analysis which is in progress.

1. P. Möller et al. Z. Physik A323, 41 (1986)
2. P. Armbruster, Preprint GSI-86-56 (1986)
3. S. Cwiok et al. Nucl. Phys. A410, 254 (1983)
4. S. Cwiok et al. Nucl. Phys. A444, 1 (1985)
5. P. Armbruster, Ann. Rev. Nucl. Part. Sci. 35, 135 (1985)
6. E. Jäger et al., contribution to this report

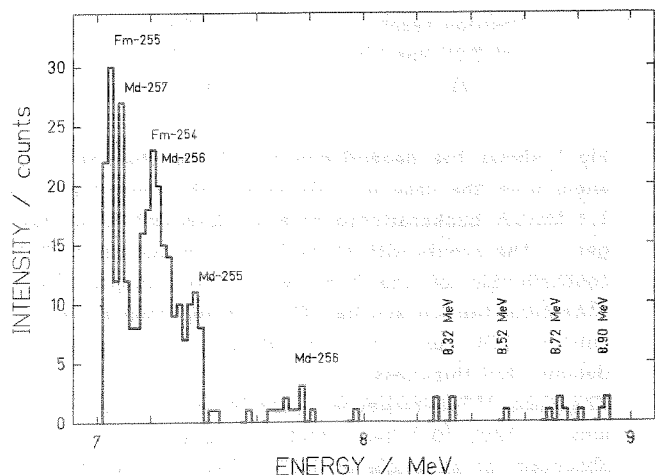


Fig. 1. Alpha-spectrum from 93 MeV $^{16}\text{O} + ^{254}\text{Es}$ after a gas-phase chemistry for element 107. Only small amounts ($\leq 10^{-3}$) of Fm and Md isotopes are not retained in the chemistry.

Search for Exotic Heavy Nuclei Using Rutherford Backscattering ^B

K.Lützenkirchen and S.Polikanov, GSI Darmstadt

G.Herrmann, M.Overbeck, and N.Trautmann, Universität Mainz

A.Breskin, R.Chechik, and Z.Fraenkel, Weizmann-Institute Rehovot

A search for exotic heavy nuclei possibly existing in nature is being carried out by means of Rutherford backscattering. As candidates for such exotic heavy nuclei we mention

- (i) nuclei containing heavy particles (mass $10 - 10^6$ GeV) produced in the early hot universe /1/,
- (ii) 'strange matter', i.e. matter composed of u,d,s-quarks in roughly equal proportions /2/, and
- (iii) transuranic nuclei with $A=300$ amu which may be stabilized against spontaneous fission through the attachment of a light ($A<1$ GeV) elementary particle.

The aim of the experiment is to investigate low-energy heavy-ion backscattering ($E/A = 1.4$ MeV/u) from various natural samples. The scattered ions are detected by means of low-pressure Multi-Wire-Proportional-Counters (MWPC) /3/. The detection system will consist of four 9×21 cm² position-sensitive Start-detectors placed around the target, and eight 28×28 cm² position-sensitive Stop-detectors installed at a 50 cm distance. The Stop-detectors contain an additional ΔE -section to measure the specific ionization.

With both Start- and Stop-detectors being position-sensitive, it is possible to perform a track reconstruction of the detected particle, and to check whether it originates from the target. Measuring both time-of-flight (TOF) and ΔE enables us to separate scattered ions from fission fragments (spontaneous fission) and from beam-impurities (see below).

A prototype of the detection system, consisting of a Start- and a Stop-detector, has been tested with ⁷⁴Ge- and ²⁰⁸Pb-beams using a thin (200µg/cm²) ¹⁹⁷Au- and a thick Monazite-target. The measured characteristics are :

- Position resolution : 0.7 mm FWHM
- Local TOF-resolution : 1.5 ns FWHM
- ΔE -resolution : 17% FWHM

Fig.1 shows the dependence of TOF on the scattering angle θ in the case of ⁷⁴Ge-ions with incident energy 1.4 MeV/A backscattered from a 200µg/cm² ¹⁹⁷Au-target. The events with short TOF correspond to a $\approx 0.2\%$ contamination of the beam with $A=40$ amu, probably ³⁸Ar from the ion source. The line represents the calculated TOF for ³⁸Ar, including corrections for the detector foil thickness.

The same ¹⁹⁷Au-target was also irradiated with ²⁰⁸Pb-ions. With 10^{13} beam particles no single event was observed at an angle of 130° . This indicates that no severe problems should arise for the planned experiments due to multiple scattering.

Fig.2 shows the ΔE -versus-TOF dependence for the scattering of ⁷⁴Ge on a thick Monazite target. The irradiation time was 16 hours at an average ion-current

of 1 particle-nA. For illustrating where to expect ⁷⁴Ge-events scattered from heavy matter inside the Monazite target, we added Part ① which is taken from the run ⁷⁴Ge + ¹⁹⁷Au at $\theta=30^\circ$, as well as three arrows. They indicate the TOF of the beam and of ⁷⁴Ge backscattered from nuclei with masses $A=300$ and $A=1000$ amu. The forementioned beam contamination, ②, (see Fig.2) does not produce a background in these regions. From Fig.2 we can calculate an upper limit for the concentration of anomalously heavy nuclei in Monazite. Most of the events in Fig.2 are ⁷⁴Ge-ions backscattered from ²³²Th and ²³⁸U. Assuming one measured event from an anomalously heavy nucleus, and taking into account the concentrations of Th, U and rare earth elements in our particular Monazite /4/, we obtain an upper limit of 10^{-8} relative to the number of rare-earth nuclei. Accordingly, this gives an upper limit for the concentration of superheavy relic particles (hypothesis (i)) of $3.5 \cdot 10^{-11}$ relative to the total number of nucleons in the target.

- /1/ J.Ellis et al., Nucl.Phys.B177 (1981) 427
- /2/ E.Witten, Phys.Rev.D30 (1984) 272
- /3/ A.Breskin et al., Nucl.Instr.Meth.217 (1983) 107
- /4/ R.Stakemann, Diplomarbeit, Univ. Mainz (1977)

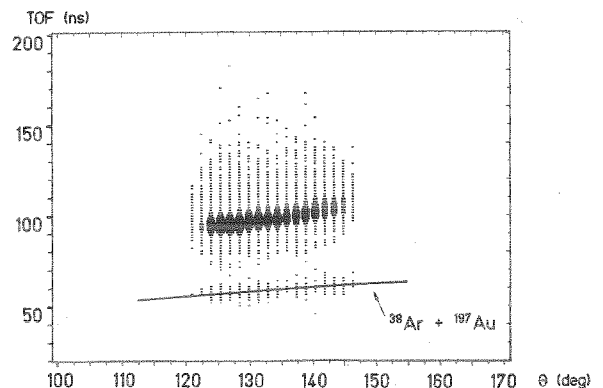


Fig.1: Time-of-flight TOF versus scattering angle θ for ⁷⁴Ge + ¹⁹⁷Au around $\theta=135^\circ$ at 1.4 MeV/u. The line is the calculated TOF for ³⁸Ar + ¹⁹⁷Au.

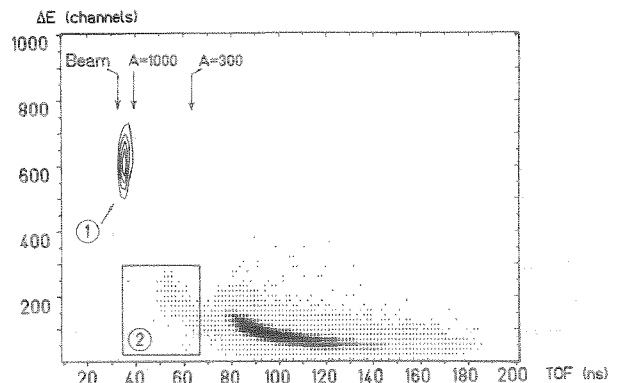


Fig.2: Energy loss ΔE versus TOF for ⁷⁴Ge + Monazite around $\theta=135^\circ$ at 1.4 MeV/u.

Evidence for Quasi-fission in the $^{40}\text{Ar} + ^{208}\text{Pb}$ Collisions
near the Coulomb-Barrier ^B

H. Keller, K. Lützenkirchen, J.V. Kratz
Institut für Kernchemie der Universität Mainz

W. Brüchele, G. Wirth, K. Sümmerer
GSI Darmstadt

Forward-backward asymmetric fission fragment angular distributions in collisions of ^{50}Ti , ^{56}Fe and ^{208}Pb near the barrier have indicated¹ that only a tiny fraction of these events originate from fission of a completely fused system inside the fission barrier. As predicted by the extra-push model^{2,3} fusion is replaced in these reactions by a new reaction channel - termed quasi-fission - which approximately equilibrates the mass asymmetry and energy degrees of freedom without ever forming a compound nucleus.

Even for lighter systems such as ^{24}Mg , ^{28}Si and $^{32}\text{S} + ^{208}\text{Pb}$ it was suggested⁴, based on the observation of unusually large angular anisotropies, that quasi-fission was contaminating the compound-nucleus fission fragment angular distributions, thus lowering⁴ the empirical threshold x_m^{thr} from about 0.7^{5,6} to 0.63. For the in-

intermediate system $^{40}\text{Ar} + ^{208}\text{Pb}$ this new parametrization⁴ would predict an extra-extra push of the order of 10 MeV, at variance with the results of an analysis⁵ of evaporation residue cross sections and of the fission excitation function in this reaction, where no evidence for a dynamical hindrance of fusion was found.

We have measured angular distributions of fission-like fragments with specific charges in the $^{40}\text{Ar} + ^{208}\text{Pb}$ reaction at $E_{\text{cm}} = 156$ and 172 MeV using catcher foil

techniques and K-Xray spectroscopy⁷. The cross sections $d^2\sigma/dZd\theta$ are symmetric around $\theta=90^\circ$ over a wider range of charge numbers as compared to the ^{50}Ti or ^{56}Fe bombardments, however, with increasing charge asymmetry, left-right asymmetries around $\theta=90^\circ$ become visible⁷. This proves that, even for $^{40}\text{Ar} + ^{208}\text{Pb}$ collisions near the barrier, quasi-fission competes with true compound-nucleus fission. This is corroborated by the angular distributions for the near-symmetric charge splits that are a factor of 2 larger than predicted by the standard saddle-point model.

In order to estimate from the differential angular distributions $d^2\sigma/dZd\theta$ what fraction of the total fission yield is due to compound-nucleus fission we have decomposed the angular distributions into an equilibrium component as given by the standard model and a quasi-fission component characterized by formulae given in Ref.1. For symmetric charge splits the relative yield for compound-nucleus fission is close to 50%; it decreases for more asymmetric splits to smaller values, e.g. $1\% \leq x_{\text{CN}} \leq 25\%$ at $Z=72$, thus indicating that the

mass(charge) distribution for the quasi-fission reaction is wider than that for compound-nucleus fission. The integral, relative yield for compound-nucleus fission results as $15\% \leq x_{\text{CN}} \leq 49\%$, and the limiting angular momentum as $22h \leq l_{\text{CN}} \leq 39h$. In the framework of the extra-push model³ this is equivalent to an extra-extra push energy for compound-nucleus formation inside the true fission saddle point of $4 \leq E_{\text{xx}} \leq 9$ MeV after extrapolation to $l_{\text{CN}}=0$. Fig.1a shows that this result is

consistent with the results of Ref.4. On the other hand, see Fig.1b, the evaporation residue cross sections⁵ for reactions of ^{40}Ar with Pb isotopes are compatible with unhindered fusion at the Bass-model fusion barrier. It is visible from Fig.1a and b that for systems of a given scaling parameter $x_m(\text{eq})$, compound-nucleus formation followed by fission is generally more severely hindered than compound-nucleus formation followed by the evaporation of particles. The $^{40}\text{Ar} + ^{208}\text{Pb}$ result of this work provides the first case in which this supposition is confirmed for the same

compound system, i.e. independently of ambiguities possibly associated with the $x_m(\text{eq})$ -scaling. Note that both sets of data refer to central collisions. For the fission data extrapolation to $l=0$ involved the scaling laws of the extra-push model. For the evaporation residue data the physical process itself restricts to central collisions. Therefore, the apparent discrepancy might point at a deficiency in the l^2 -scaling of the extra-push model.

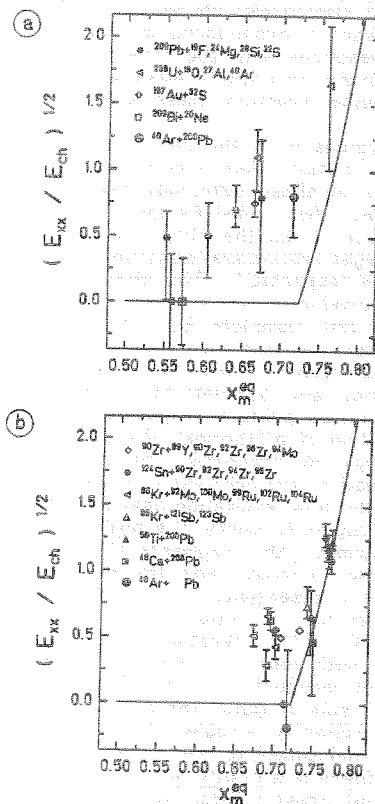


Fig.1 : a) Square root of the extrapolated dimensionless quantity $E_{\text{xx}}/E_{\text{ch}}$ for central ($l=0$) collisions as extracted⁴ from fission-fragment angular distributions vs. the system parameter $x_m(\text{eq})$. The result for $^{40}\text{Ar} + ^{208}\text{Pb}$ of this work is also indicated. b) Same systematics based on fusion-evaporation residue cross sections. The solid lines are theoretical predictions⁸ for symmetric systems within the Chaotic Regime Dynamics¹.

¹ K. Lützenkirchen et al., Z. Phys. A320, 529 (1985) and Nucl. Phys. A452, 351 (1986)
² W.J. Swiatecki, Physica Scripta 24, 113 (1981)
³ S. Bjørnholm, W.J. Swiatecki, Nucl. Phys. A391, 471 (1982)
⁴ B. B. Back, Phys. Rev. C31, 2104 (1985)
⁵ H. Gägeler et al., Z. Phys. A316, 291 (1984)
⁶ C. C. Sahm et al., Nucl. Phys. A441, 316 (1985)
⁷ H. Keller et al., GSI Scientific Report 1985, GSI 86-1, p.70, (1986)
⁸ J. P. Blocki et al., Preprint GSI 86-16, (5/1986)

Unusual Excitation-Energy Division in Quasi-Fission Reactions between
 ^{50}Ti , ^{54}Cr and ^{58}Fe with $^{207,208}\text{Pb}$
 at the Barrier ^{G,B}

H. Keller, R. Bellwied, K. Lützenkirchen^a, J.V. Kratz
 Institut für Kernchemie der Universität Mainz

W. Bröchle, H. Gaggeler^b, K.J. Moody^c, M. Schädel, K. Sümmerer,
 G. Wirth
 GSI Darmstadt

We have measured mass- and charge distributions for quasi-fission in the reaction of 4.85 MeV/u ^{50}Ti with ^{207}Pb , 4.90 MeV/u ^{54}Cr with ^{208}Pb , 5.02 MeV/u ^{58}Fe with ^{208}Pb , and 5.15 MeV/u ^{58}Fe with ^{209}Bi during the respective SHIP experiments producing isotopes of elements 104, 106, 108, and 109¹. The fission products recoiling from the SHIP target after being stopped in catcher foils, were subject to extensive chemical separations and low level γ -ray spectroscopy.

The Z-yield curve develops from constant cross sections for all fission-like charges² for the ^{50}Ti -induced reaction toward a pronounced minimum at charge symmetry for reactions with the ^{58}Fe projectile, indicating a progressively incomplete mass asymmetry relaxation and decreasing reaction times with increasing proton number.

For fixed values of Z the centroids of the (gaussian) isotope distributions hold a surprise: Consistently, for all reactions at these extremely low bombarding energies we find that quasi-fission fragments that have been produced from the projectile by taking up mass from the target are several mass units more neutron-deficient than expected³. The data for heavy fission fragments produced by stripping nucleons from the target are less complete but there is evidence that these are more neutron-rich than expected, see Table 1. The expectations³ are based on potential energy considerations and simulations of neutron evaporation from the excited primary fragments involving the crucial assumption of a (thermal) division of the total excitation energy in proportion to the fragment masses. The data lead to the opposite conclusion concerning the division of the total excitation energy: The lightest quasi-fission fragments carry the highest excitation energies, at symmetry the fragments share equal amounts of the excitation energy, and the heaviest quasi-fission fragments are essentially cold. The fractional excitation energies as a function of Z are depicted in Fig. 1 for the $^{54}\text{Cr}+^{208}\text{Pb}$ reaction. These results are in agreement with our previous observation⁴ of cold below-target products in the $^{48}\text{Ca} + ^{249}\text{Cm}$ reaction. Thus, both sets of data, the present one and those of Ref. 4, consistently suggest the following mechanism: For the initial phase of the mass drift from target to projectile there is a highly ordered transfer of nucleons from the outermost orbitals of the target nucleus into unoccupied orbitals in the projectile, leaving a cold core of the target nucleus and a projectile-like acceptor nucleus with as many particle-hole excitations as particles were transferred. With increasing mass drift (i.e. >10 protons and >30 neutrons) the initially highly ordered, one-directional mass flow gets increasingly randomized, so that an equal share of the total excitation energy is gradually approached.

Such an unusual, extreme division of the excitation energy between two fragments goes far beyond previous evidence for temperature nonequilibrium in deep-inelastic collisions⁵⁻⁷ or quasielastic collisions⁸ of systems with similar entrance channel mass asymmetry studied at much higher energies.

In the present experiments performed at the Bass-model fusion barrier projectile and target are brought together in central collisions with zero relative velocity. The initial absence of randomization in these smooth encounters of two nuclei may be associated with the non-availability of collective kinetic energy for dissipation.

Z	^a <A> _Z ^{prim}	^b E _{tot} [*]	^c E _Z [*]	^d <A> _Z ^{sec}	^e <A> _Z ^{sec}	^e E _Z [*]
calculated					experimental	
35	85.0	70.5	23.3	83.0	77.8	80.6
41	100.5	75.8	29.3	97.5	93.6	73.6
46	116.0	81.2	35.2	113.0	108.9	72.2
51	126.0	92.9	44.7	122.0	122.0	40.6
53	131.0	94.8	47.4	126.0	126.9	40.3
55	136.0	94.5	49.0	132.0	133.0	28.8
65	161.0	73.6	45.2	157.0	157.4	28.2
71	177.0	70.5	47.2	173.0	175.3	16.4
72	178.5	69.3	47.1	173.5	178.0	11.0

Tab.1 : Centroids of isotope distribution and fragment excitation energies in the $^{54}\text{Cr}+^{208}\text{Pb}$ reaction.

^a minima of the potential energy surface including shell effects

^b for fully relaxed total kinetic energies

^c assuming division of E_{tot}^{*} in proportion to the masses

^d calculated from ^a and ^c

^e these values are consistent with $\langle A \rangle_Z^{\text{sec}}$

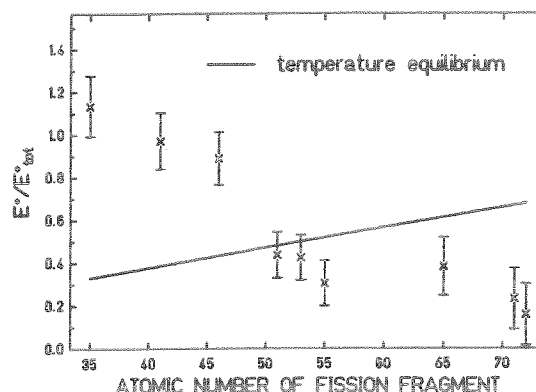


Fig.1 : Division of the total excitation energy between the two quasi-fission fragments. The solid line represents the temperature equilibrium where the total excitation energy is divided in proportion to the fragment masses. The data are for 4.9 MeV/u $^{54}\text{Cr}+^{208}\text{Pb}$.

¹ P. Armbruster, Preprint GSI-84-47 (1984)
² H. Keller, GSI Scientific Report 1984, GSI 85-1, p.36 (1985)
³ K. Lützenkirchen et al., Z. Phys. **A317**, 55 (1984)
⁴ H. Gaggeler et al., Phys. Rev. **C33**, 1983 (1986)
⁵ T.C. Awes et al., Phys. Rev. Lett. **52**, 251 (1984)
⁶ R. Vandenbosch et al., Phys. Rev. Lett. **52**, 1964 (1984)
⁷ H. Breuer et al., private communication
⁸ H. Sohlbach et al., GSI Scientific Report 1984, GSI 85-1, pp.56-57 (1985)

^a presently at GSI Darmstadt
^b presently at EIR Würenlingen
^c presently at LLNL Livermore

Nuclear Reactions and Nuclear Contact in U+U Collisions below the Barrier ^B

G. Wirth, W. Brüche, Fan Wo, K. Sümmerer
 GSI Darmstadt
 F. Funke, J.V. Kratz, N. Trautmann, M. Lerch
 Institut für Kernchemie, Universität Mainz

Positron line structures in U+U collisions at energies near the Coulomb barrier have attracted considerable interest. Experimentally it seems not to be excluded that nuclear contact plays a role. The calculation of the nucleus-nucleus potential is difficult due to the deformation of the U nuclei. We have therefore looked for nuclear reaction products as probes for nuclear overlap. One-neutron transfer which is the most probable direct reaction does not prove nuclear contact since we have observed it still at a distance of closest approach of 24 fm, which is rather large compared with the strong interaction radius of 16.7 fm. Some information on the nucleus-nucleus potential may be contained in the deviations of the one-neutron transfer probability from an exponential behaviour for the most central collisions¹.

In order to assess possible reasons for these deviations angular distributions of the 1n-transfer products were measured in the much less deformed but also symmetric system ¹⁹⁷Au + ¹⁹⁷Au at beam energies of 5.06 (0.88 × B) and 5.35 (0.93 × B) MeV/u. Both angular distributions do not show the pronounced bending near $\Theta_{CM} = 180^\circ$ as observed in ²³⁸U + ²³⁸U collisions. However, a plot of all transfer probabilities from the angular distributions in the reaction ¹⁹⁷Au + ¹⁹⁷Au (fig. 1) does not have the expected strict exponential dependence on d_0 . Agreement with the theory is obtained if only the transfer probabilities within the angular range $90^\circ \leq \Theta_{CM} \leq 115^\circ$ are taken. This fit is shown as solid line in fig.1 and the slope $2\alpha = 1.18 \text{ fm}^{-1}$ coincides with the expected value $2\alpha = 1.19 \text{ fm}^{-1}$ deduced from the ground-state binding energy of the transferred neutron. As a consequence the differential cross sections for the more central collisions are somewhat lower than predicted by the theory. This is qualitatively similar to the observation in the system ²³⁸U + ²³⁸U although the effect is much less pronounced in ¹⁹⁷Au + ¹⁹⁷Au. To confirm this preliminary result we need the angular distributions in the reaction ¹⁹⁷Au + ¹⁹⁷Au at two additional energies. It remains open whether the shape of the angular distributions for the one-neutron transfer contains detailed information on the nucleus-nucleus potential.

Fission is, as one-neutron transfer, not an indication of nuclear contact since we have measured quite high cross sections for Coulomb fission induced by the long range Coulomb forces². The transfer of many nucleons between two U nuclei requires a window or a neck and may serve as an experimental signal for nuclear contact during the collision. We have observed the 2p9n transfer product ²²⁷Th in U + U collisions at a beam energy of 5.85 MeV/u and at the laboratory angle $\Theta = 45^\circ$ (fig. 2). This shows that under kinematical conditions where peak structures

in the positron spectra have been observed U + U collisions occur with massive nuclear overlap. The excitation function for ²²⁷Th is much steeper than for one-neutron transfer. A comparison of the excitation functions of positron peaks and multinucleon transfer for different systems may help to clarify the role of nuclear contact for the positron lines.

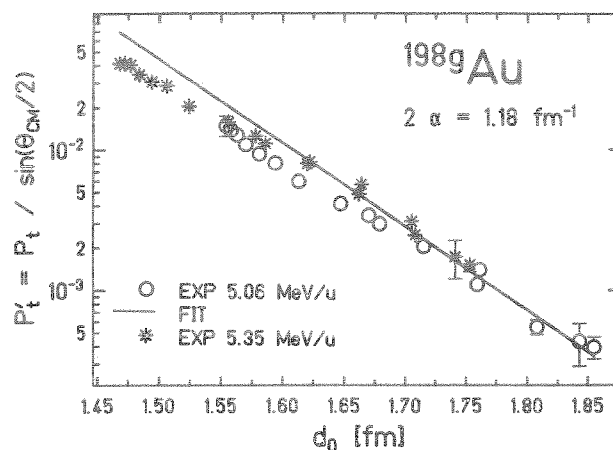


Fig.1: Transfer probabilities for ^{198g}Au in ¹⁹⁷Au + ¹⁹⁷Au at bombarding energies 5.35 and 5.06 MeV/u.

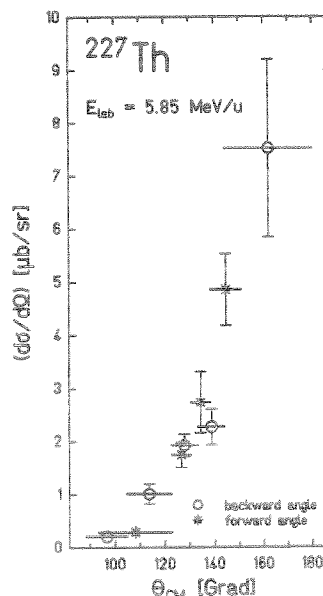


Fig.2: Angular distribution for ²²⁷Th in ²³⁸U + ²³⁸U at $E_{LAB} = 5.85 \text{ MeV/u}$.

References:

1. G. Wirth et al., Phys. Lett. **177B** (1986) 282
2. G. Wirth et al., GSI 86-1, 59 (1986)

Fragmentation in the System $^{197}\text{Au} \rightarrow ^{197}\text{Au}$ at 15 MeV/u^B

Th. Blaich, J.V. Kratz, R. Schmoll
 Institut für Kernchemie, Universität Mainz

K. Sümmerer, G. Wirth
 GSI Darmstadt

We have previously reported¹ on the production of medium heavy fragments (MHF) in the mass range $20 \leq A \leq 40$ in the system $^{197}\text{Au} \rightarrow ^{197}\text{Au}$ at bombarding energies ≤ 15 MeV/u. We showed that production of MHF in the first, binary step of a deeply inelastic collision (DIC) can be ruled out and that other mechanisms must be considered, e.g. sequential fission of a gold-like heavy fragment or many-body breakup-reactions. The latter are conceivable because in the first reaction step maximum excitation energies of 500 MeV per gold-like fragment are reached, and this value exceeds the Q-value of a breakup-reaction by a factor of two.

^{197}Au -targets were irradiated in a cylindrical scattering chamber, and the reaction products were collected in stacks of catcher foils and identified by off-line γ -spectroscopy. We obtained crude angular distributions (front, rear side and mantle of the scattering chamber) and range distributions in the forward direction. Summation of the cross sections observed in the foils yielded integral production cross sections which were used to reconstruct the mass and charge distribution of the reaction products.

The experimental distributions of the MHF among the catcher foils were compared to theoretical ones which were calculated under the assumption that the MHF originate from sequential fission of a gold-like product of a binary DIC. The calculations were performed with a schematic model which was developed by Glässel et al.² and is able to reproduce their data on sequential fission in the system $^{129}\text{Xe} + ^{122}\text{Sn}$ at 12.5 MeV/u. We considered two cases: equilibrium fission and fast fission with proximity effect as observed in ref. 2. The latter reproduces the data for $35 \leq Z \leq 45$. However, both cases fail to describe the MHF data, as is shown in fig. 1: Equilibrium fission predicts too large cross sections at high velocities in the forward direction and on the rear side of the scattering chamber (hatched area in fig.1.a). These shortcomings do not depend on details of the model, e.g. spin of the fissioning system or the time interval between the reaction steps, but can only be overcome by assuming fast fission with extremely asymmetric angular distributions of the fission products. These assumptions, however, predict high cross sections in the vicinity of the cm-velocity (hatched area in fig.1.b), which are not found in the data.

Alternatively, the MHF data were compared to the predictions of the breakup model by Aichelin et al.³ Fig. 2 shows the result: The experimental distribution is reasonably described, without adjustment of any parameters at all. Thus, the relative distributions of the MHF among the catcher foils indicate that these nuclei are not formed by sequential fission in a three-body reaction but by a process with higher multiplicity of the reaction products.

The large absolute cross sections for MHF point to the same conclusion: they are about twice as large as conservative estimates for sequential fission, even if fission of both products of the first step is taken into account. Within the breakup model, however, it is possible to reproduce the high element yields near $10 \leq Z \leq 15$ with an integral cross section for breakup of only 180 mbarn. This is due to the high multiplicities predicted by

ref. 3. Comparison of this rather small cross section to the reaction cross section of 4.8 barn indicates that this mechanism is restricted to the most central collisions, as expected. Also, the flat element distribution can be qualitatively reproduced⁴ as a superimposition of a breakup distribution (decreasing cross sections for increasing Z with very small cross sections beyond $Z \approx 20$) and a broad fission product distribution with a maximum near $Z \approx 38$.

It is tempting to conclude that MHF in the system $^{197}\text{Au} \rightarrow ^{197}\text{Au}$ at 15 MeV/u are not produced in sequential fission, but in a process which resembles the cold breakup as defined in ref.3, i.e. a mechanism with rather high multiplicity of reaction products.

References:

- /1/ Th. Blaich et al., GSI Scientific Report 1983, GSI 84-1, p.33(1984)
- /2/ P. Glässel et al., Z.Phys. **A310**,189(1983)
- /3/ J. Aichelin et al., Phys.Rev. **C30**,107(1984)
- /4/ Th.Blaich, doctoral thesis, University of Mainz 1987

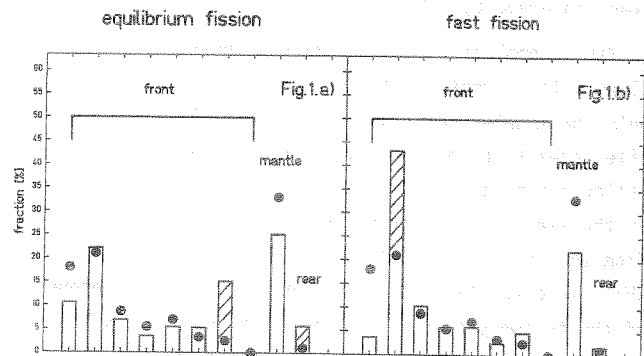


Figure 1: Relative distributions of ^{28}Mg among the front (range distribution), the mantle and the rear of the scattering chamber. The circles represent the experimental data, whose errors are smaller than the diameters of the circles, and the columns represent theoretical distributions.

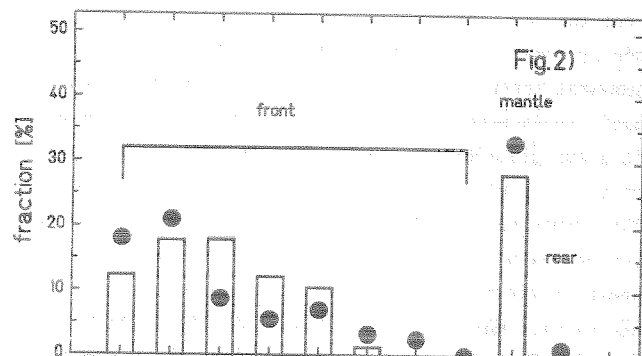


Figure 2: Relative distributions of ^{28}Mg . The meaning of the symbols is the same as in fig.1.

The Deflection Function for the Reaction $^{197}\text{Au} \rightarrow ^{197}\text{Au}$ at 15 MeV/u ^B

R. Schmoll, Th. Blaich, J.V. Kratz
 Institut für Kernchemie, Universität Mainz
 K. Sümmerer, G. Wirth
 GSI Darmstadt

In preceding experiments [1,2] we investigated the reaction mechanism for the production of medium heavy fragments MHF ($10 \leq A \leq 40$) in the system $^{197}\text{Au} \rightarrow ^{197}\text{Au}$ at bombarding energies of 9,11,13 and 15 MeV/u. Up to now, the production of MHF has been associated with several mechanisms. A first inclusive experiment [3] suggested a dynamical splitting of the projectile while data from subsequent experiments have been successfully interpreted as a true two-step mechanism with fission probabilities compatible with expectations from the statistical model [4]. Three-body exclusive experiments [5] confirmed the two-step nature of these sequential, fission-like reactions, however, they established a fast time scale for the sequential fission such that both angular and velocity distributions of the fission fragments were modified by a Coulomb final state interaction due to the proximity of the partner of the first, deep-inelastic reaction step. It was also shown [5] that these pre-equilibrium processes have a tendency for asymmetric mass splits.

Our data [2] for the reaction $^{197}\text{Au} \rightarrow ^{197}\text{Au}$ at 15 MeV/u seem to indicate a similar proximity effect. For a realistic simulation of the three-body or four-body Coulomb trajectories in these collisions it was essential to know the deflection function for Au-like fragments because the deflection angle as a function of TKE would also tell us the locus of the source of sequential fission fragments. Hence, we have measured the deflection function in an additional one-body inclusive experiment in the reaction $^{197}\text{Au} \rightarrow ^{197}\text{Au}$ at 15 MeV/u. The reaction products with atomic numbers ranging from $35 \leq Z \leq 79$ have been implanted in a stack of 10 catcher foils which covered the angular range $3.5 \leq \Theta \leq 35$ degrees in the lab frame. Fig. 1 shows the velocity diagram for gold. The catcher foil positions are indicated by their limiting laboratory angles and limiting velocities. The latter are derived from range-velocity relations. After the bombardment the catcher foils were cut into pieces representing 3.5° slices of laboratory angles and measured by off-line KX-ray spectroscopy. From the distribution of the KX-ray activities in the catcher foils we deduced the centroids of the distributions in the v_{lab}, Θ_{lab} -space for every Z . The data shown in Fig. 2 display the locations of the centroids of TKE versus CM deflection angle distributions for all measured Z . Nuclear reactions begin with very low energy loss and large cross sections for neutron exchange processes. Increasing TKEL is then associated on the average with an increasing loss of charge. This is due to a depletion of the higher charges both by sequential fission and charged-particle evaporation. For all energy losses including the completely relaxed events, corresponding to an energy loss of ≥ 1 GeV the cross sections are rather sharply peaked at the grazing angle $\Theta_{gr} = 27^\circ$. Even at the highest energy losses the binary process remains the dominant reaction channel. Fig. 3 shows the angular distribution at different TKE, $480 \leq TKE \leq 1450$ MeV, and exhibits the familiar broadening of the angular distribution for increasing TKEL. The FWHM reaches $\approx 30^\circ$ for completely damped events reflecting strong focussing over the whole range of TKEL.

For $Z \leq 47$, the well developed grazing peak vanishes. Fig. 4 shows the KX-ray intensity distribution for $Z = 35$ in the velocity space exhibiting a Coulomb-hole as a clear pattern of fission.

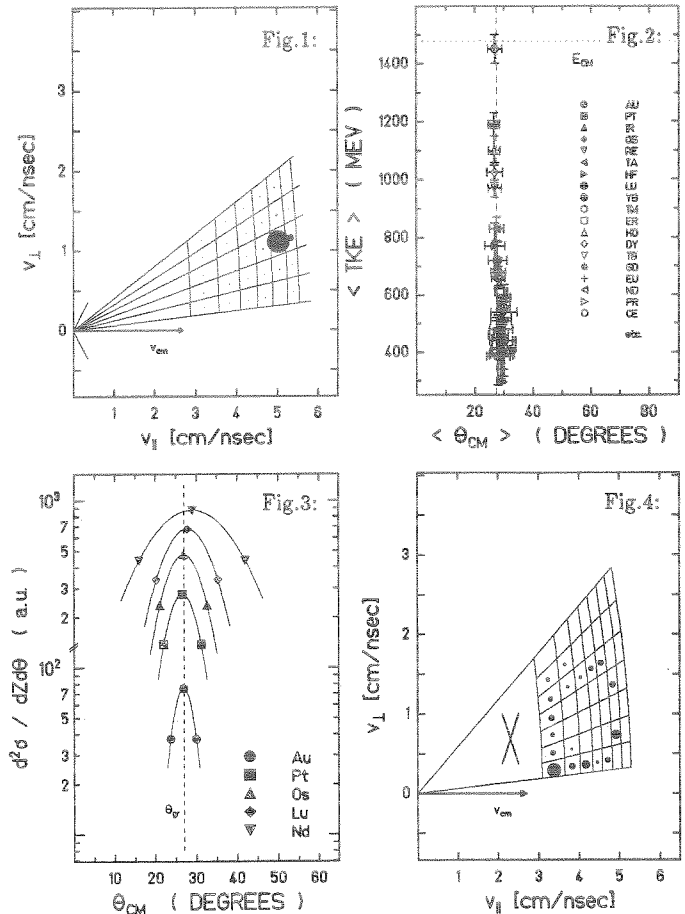


Figure 1: Velocity diagram for $Z = 79$. Each catcher foil is characterized by a triangular or quadrangular area in the laboratory angle versus lab velocity field. The black filled circles shown in each of these fields scales with the measured cross section.

Figure 2: Wilczynski-plot for the system $^{197}\text{Au} \rightarrow ^{197}\text{Au}$ at 15 MeV/u for binary events.

Figure 3: Angular distributions at different TKE. The dashed line indicates the grazing angle.

Figure 4: Velocity diagram for $Z = 35$. The diameter of the black circles scales with the detected cross section.

References

- [1] Th. Blaich et al., GSI Scientific Report 1983, GSI 84-1, p.33(1984)
- [2] Th. Blaich et al., this report
- [3] A. Olmi et al., Phys.Rev.Lett.44, 383(1980)
- [4] T.C. Awes et al., Phys.Rev.Lett.55, 1062(1985)
- [5] P. Glässel et al., Z.Phys. A310,189(1983)

An On-Line Chemistry for Element 107

E. Jäger, M. Schädel
GSI Darmstadt

To search for isotopes of element 107 in radiochemical experiments with ^{254}Es as a target¹ an on-line chemical separation of element 107 (Eka-Rhenium), especially from the actinide elements is needed. Isotopes of element 107 are expected to be produced with cross sections of only about 1 nb or even less. The estimated half-lives for α - and EC-decay are between 0.1 and 10 minutes. We developed on-line separations in the gas-phase in close analogy to the experiments carried out in Dubna by Domanov, Zvara and coworkers²⁻⁴. The separation is based on the volatility of the platinum metal oxides.

We have optimized our chemistry for element 107 with its homologue rhenium. From considerations of the systematics of chemical behaviour the 107-oxides are expected to have a similar volatility as the Re-oxides have³.

In a first series of off-line experiments we irradiated ReO_3 powder with neutrons in the Mainz Triga Reactor, dissolved the oxid in nitric acid, dried aliquots in a quartz crucible and inserted it into the thermochromatography tube to start the chemistry. A temperature gradient along the quartz tube between 1050 °C and room temperature was adjusted. We studied the influence of the following parameters on the formation of different compounds and their condensation temperature in the quartz tube (position determined by γ -spectroscopic assay): He or N_2 as an inert carrier gas, flow rate of 0.75 and 1.5 l/min, O_2 content of 5 and 30% (volume), H_2O content between < 50 and > 1000 ppm, and the duration of the experiment between 1 and 30 min. Most important were the observations that (1) in a dry atmosphere (< 50 ppm H_2O) only one component at about 420 °C condensation temperature, T_c , was present, (2) in a H_2O containing atmosphere (≥ 200 ppm) a second ($T_c \cong 120$ °C) and third ($T_c < 40$ °C) component with an amount of about 50% of the total intensity was present, and (3) that these results are rather insensitive to changes of all the other parameters (time, flowrate, O_2 content) investigated. To check these results with carrier free tracer activities we produced $^{181-184}\text{Re}$ in an irradiation of a W-target with protons at the Kernforschungszentrum Karlsruhe. The Re-oxide was evaporated at 1050 °C from the W and condensed onto a Au foil which was later inserted into our thermochromatographic column to start the chemistry under the same conditions as mentioned above. From these experiments we could observe only the component at $T_c = 420$ °C on a quartz surface independent of the H_2O content in the gas. Within one minute, the shortest time used in off-line experiments, 95% of the Re was evaporated from the Au foil. In on-line experiments we are expecting to obtain separation times including the transport time of less than 3s. To find the best suited catcher material for 107-oxides on the gas outlet of the thermochromatographic columns we inserted several metal foils into the quartz tube to possibly observe an increase of the condensation temperature. While from Fe, Ti and Zr no significant changes could be ob-

served Ni and even much better Ta adsorbed the Re-oxides at higher temperatures. With a Ta-foil also the low temperature components at $T_c = 120$ °C and $T_c < 40$ °C were retained at $T_c > 200$ °C. From these experiments a 0.67 mg/cm² Ni-foil, coated with 50 $\mu\text{g}/\text{cm}^2$ Ta was selected as a catcher.

In the on-line experiments to search for $^{266}\text{107}$ the recoil products were thermalized in a He atmosphere at about 1.1 bar and were transported by a He jet containing KCl clusters with a flow rate of typically 0.75 l/min to our On-Line Gas-phase Chemistry Apparatus OLGA. A schematic drawing of the apparatus, including the temperature profile along the quartz tube in the oven system, is shown in fig. 1. All clusters are destroyed in a quartz wool plug kept at 1050 °C. A flow of 0.2 l/min O_2 was added to the He in front of the quartz wool to form a volatile oxide of element 107 while the non-volatile actinides are stopped in the quartz wool. As the water content in the gases was kept below 100 ppm we are expecting only one volatile component, the 107-trioxide, with an estimated condensation temperature in quartz at about 400 °C. The thermochromatographic column was kept above this temperature to condense the activity onto a thin, Ta-coated Ni foil facing the outlet of the quartz column. The Ni foil was cooled from the backside with He which was at liquid nitrogen temperature. The catcher foils were rotated stepwise in front of pairs of surface barrier detectors for an α -particle and sf assay. The data acquisition system normally connected to the MAD wheel⁵ was used for data accumulation. With the final set-up the chemistry was checked again with $^{176-178}\text{Re}$ from the reaction of ^{16}O with a Ho foil mounted between the ^{254}Es target and the recoil chamber. The transport efficiency was determined to be 56% and the chemistry yield including the condensation was 100%.

1. M. Schädel et al., contribution to this report
2. V.P. Domanov, I. Zvara, Radiokhimiya 26, 770 (1984)
3. V.P. Domanov et al., Report JINR P6-81-768, Dubna 1981
4. I. Zvara et al., Report JINR P6-82-616, Dubna 1982
5. R.J. Dougan et al., Report UCAR 10062/85-1 (1986) p. 4-50

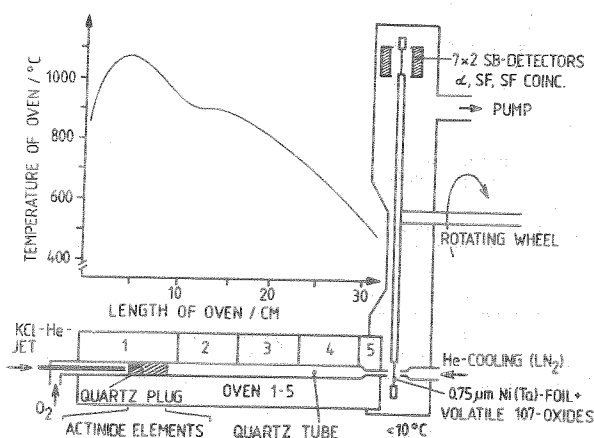


Fig. 1. The set-up for the element 107 chemistry is shown schematically in our On-line Gas Phase Chemistry Apparatus.

The Ionic Radii of Lr^{3+} and Md^{3+} Aquo Ions and their Single-Ion Heats of Hydration^B

W. Brüche, M. Schädel, B. Schausten

GSI Darmstadt

J.V. Kratz, U.W. Scherer

Institut für Kernchemie, Universität Mainz

R. Henderson, R. Chasteler, H. Hall, K.E. Gregorich, D.C. Hoffman,

D. Lee, M. Nurmia

Lawrence Berkeley Laboratory

The only chemical experiments with lawrencium (Lr) performed to date by Silva et al.¹ indicated a stable trivalent oxidation state in aqueous solutions. Since Lr seemed to behave like its lighter homolog, lutetium, it was assigned the last member of the actinide series with ground state electronic configuration $5f^{14}7s^26d^2$. Brewer², however, predicted a different configuration caused by relativistic effects, $5f^{14}7s^27p_{1/2}$, corroborated by Dirac-Fock calculations³. The trivalent oxidation state could result from either configuration leaving an intact $5f^{14}$ core. Relativistic effects could be reflected in thermodynamic properties e.g. the heat of formation (ΔH_f). This complex quantity can be broken with the aid of the Born-Haber cycle into more simple components⁵: the heat of sublimation (ΔH_{sub}), the ionization energy (ΔH_{IP}), and the heat of hydration (ΔH_{hyd}). The first can be measured by gas chromatography, the ionization energy can only be calculated presently. The latter can be deduced from the ionic radius via the determination of the elution position from a chromatographic system. The elution position is related to the distribution coefficient K_D between the mobile and stationary phase. For equally charged ions of the same coordination the $\log K_D$ is linearly dependent on the ionic radius⁵.

^{260}Lr ($T_{1/2} = 3$ min) and lighter actinides were produced at the LBL 88-inch Cyclotron by bombarding a ^{249}Bk target with ^{18}O ions. Products recoiling from the target were transported by a Helium-jet to the surface of a frit in the head of the microprocessor - controlled Automated Rapid Chemistry Apparatus, ARCA⁷. After 10 min accumulation time these products were dissolved in 0.05 M α -hydroxy-isobutyric acid (HIBA) of pH = 4.85 and loaded on top of a cation exchange column (2.0 x 60 mm) packed with Aminex A6 resin. During the loading procedure the jet was bypassed, and tracer activities (^{171}Tm , ^{171}Er , ^{168}Ho) were added. Then the reaction products and tracers were eluted from the column with 0.12 M HIBA at pH = 4.85. Fractions of increasing volume were collected on tantalum disks, evaporated to dryness and flamed before transferring them to the counting system. After the elution of Ho the column was stripped with 0.5 M HIBA at pH = 4.85 and regenerated. Setting up ARCA as a symmetrical twin system with two cation exchange columns allowed for a high repetition rate by processing both columns alternately.

The 10 samples of each run were counted for α -particles immediately after the elution in an array of 10 Si(Au) surface barrier detectors. The average time difference between end of the collection and start of the counting was $\Delta t \approx 3$ min for the samples containing Lr. ^{260}Lr was detected in the α -particle spectra as single events at 8.03 MeV. Their time distribution is compatible with a half-life $T_{1/2} = 126^{+44}_{-18}$ s. The distribution of the lanthanide tracer activities was monitored afterwards by γ -ray counting with two Ge(Li) detectors.

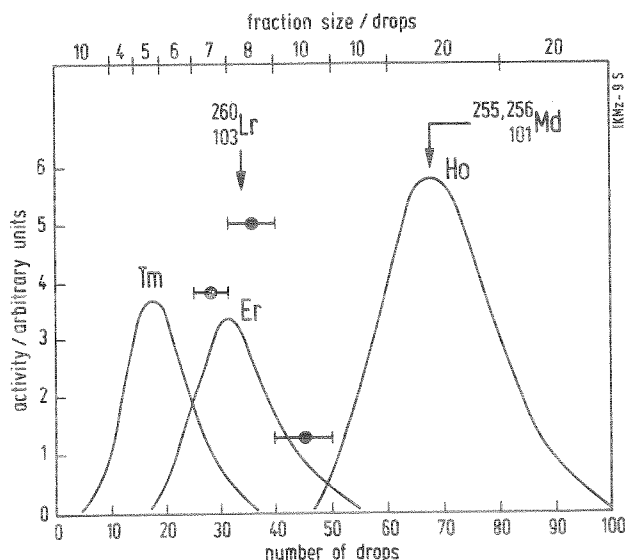
In 93 chemical separations we were able to detect 25 decays of ^{260}Lr . A preliminary data analysis of the first eight events (figure) shows the elution position of Lr almost coinciding with the position of Er. In addition to the peaks of the other tracers the figure also indicates the elution position of mendelevium. The known correlations of the elution positions of the lanthanide tracers with their ionic radii enabled us to determine the ionic radii of the two actinide ions by interpolation. Preliminary results are $r \approx 0.882 \text{ \AA}$ for Lr^{3+} and $r \approx 0.896 \text{ \AA}$ for Md^{3+} in agreement with recent empirical predictions⁵. By inserting these values into the semiempirical Phillips - Williams equation⁹

$$\Delta H_{\text{hyd}} = - \frac{7.32 z^2}{r + 0.85} \text{ eV}$$

(with the oxidation state $z = 3$) one can calculate the single ion heats of hydration, which result as $\Delta H_{\text{hyd}} \approx 38.2 \text{ eV}$ for Lr^{3+} and $\Delta H_{\text{hyd}} \approx 38.0 \text{ eV}$ for Md^{3+} .

1. R. Silva et al. Nucl.Chem Letters 6,733 (1970)
2. L.J. Nugent et al. Phys. Rev. A9, 2270 (1974)
3. L.J. Brewer J.Opt.Sci.Am. 61,1101(1971)
4. J.P. Desclaux et al. J.Physique 41, 943 (1980)
5. O.L. Keller Radiochim.Acta 37, 169 (1984)
6. Y. Marcus, A.S. Kertes "Ion Exchange and Solvent extraction of Metal Complexes", Wiley Interscience New York 1969, p.287
7. W. Brüche et al. GSI Scientific Report 83 GSI 84-1 (1984) p.247
8. S.G. Bratsch, J.J. Lagowski J.Phys.Chem. 90/2, 309 (1986)
9. C.S.G. Phillips, R.J.P. Williams "Inorganic Chemistry", Oxford University Press, London 1965 vol.2, p.160

Figure: Elution of ^{171}Tm , ^{171}Er , ^{168}Ho tracer activities (curves) and of ^{260}Lr (data points) from a cation exchange column (2.0 x 60 mm) with 0.12 M HIBA.



Lawrencium: No Evidence for Lower Oxidation States than 3+ in Aqueous Solution^B

U.W. Scherer, J.V. Kratz, N. Trautmann, S. Zauner
 Institut für Kernchemie, Universität Mainz
 M. Schädel, W. Brüchele
 GSI Darmstadt
 K.E. Gregorich, D.C. Hoffman, D. Lee, M. Nurmia
 Lawrence Berkeley Laboratory

Lawrencium, element 103, is the last member of the 5f actinide series and its chemistry should be similar to that of its lighter homolog, lutetium. One would then expect that the ionization would stop with the 5f¹⁴ core intact, giving rise to a stable trivalent oxidation state of Lr. Silva et al.¹ in the only chemical experiments with Lr performed to date have confirmed this valence state.

Lawrencium was traditionally expected to have a 5f¹⁴6d7s² electronic configuration although Brewer² predicted a 5f¹⁴7s²7p configuration. The latter has been confirmed by multidimensional relativistic Dirac-Fock calculations³ where the new ground state configuration results from strong relativistic effects on the 7p_{1/2} orbital. Furthermore, Brewer has pointed out that the 7s² closed shell itself might be sufficiently contracted and stabilized by relativistic effects making it an 'inert core' so that only the 7p_{1/2} electron may ionize under reducing conditions to produce monovalent Lr¹⁺.

We have searched for this unusual oxidation state in aqueous solutions using Cr²⁺ and V²⁺ metal ion as reductants. In case of the reduction of Lr³⁺ to Lr¹⁺ the ions become larger and have obviously less charge. This can be made visible by extraction chromatography with di(2-ethylhexyl)orthophosphoric acid (HDEHP) for which the affinity for metal ions depends sensitively on the size and charge of the ion.

The 3 min isotope ²⁶⁰Lr and lighter actinides were produced at the Lawrence Berkeley Laboratory 88-inch Cyclotron in transfer reactions between ¹⁸O and ²⁴⁹Bk. The reaction products recoiled into a volume of He gas saturated with an KCl aerosol. The Helium-jet transported the activities into the head of an Automated Rapid Chemistry Apparatus, ARCA⁴ where the aerosols together with the reaction products were collected on the surface of a quartz frit. The collected activity was processed batchwise after 9 min accumulations. This involved the dissolution of the activities from the frit in 0.3 M HCl containing 0.01 M V²⁺ or Cr²⁺ as reducing agents and pumping this solution over a first HDEHP column (1.75 x 40 mm) where monovalent and divalent ions passed through while the trivalent actinides were strongly absorbed on top of the column. The effluent from the first HDEHP column was contacted with H₂O₂ so that the reduced actinides were re-oxidized (except for No) to the trivalent state. These were fixed on a second HDEHP column which was subsequently washed to remove No²⁺ and the oxidized chromium and vanadium metal ions. Both columns were then stripped with 4 M HCl, and the eluting actinides in both cases were collected on tantalum disks, evaporated to dryness and counted for α -activities. Counting of the samples started 3 min after the end of bombardment. The microprocessor - controlled Chemistry Apparatus then reconditioned the HDEHP columns. Simultaneously, new activity had been collected since washing of the frit was finished. When the columns were in the initial state a new separation cycle was started automatically.

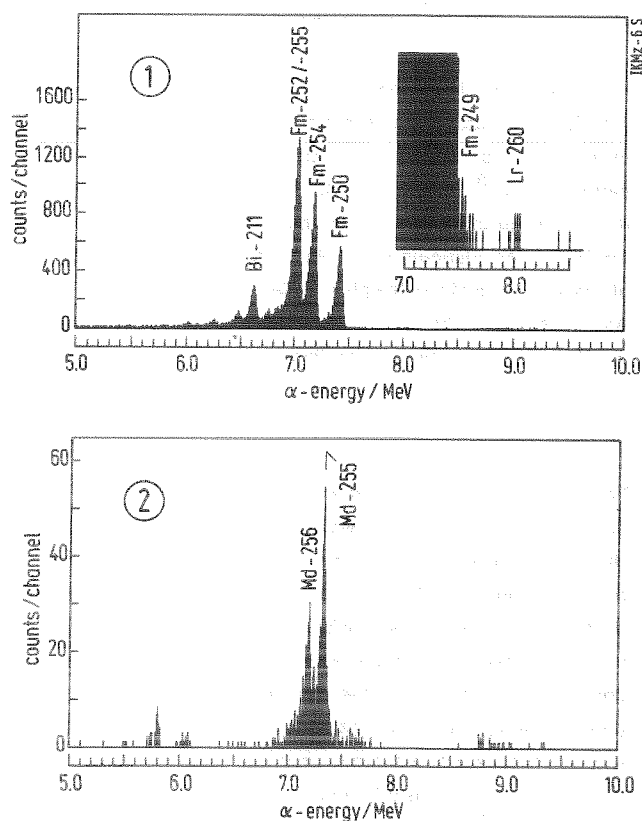
The figure shows the sum of the α -particle spectra from 30 runs with Cr²⁺ as reductant. In the unreduced fraction, besides large activities of several Fm isotopes there are 13 events with energies compatible within resolution with the 8.03 MeV α -energy of ²⁶⁰Lr and with a time distribution compatible with its 3 min half-life. The reduced fraction, on the other hand, contains the Md products in the 2+ state, as expected⁵, but no ²⁶⁰Lr, since we could not detect a single α -particle in the energy range between 7.9 and 6.5 MeV. Obviously, we were not able to reduce Lr even with the stronger reductant Cr²⁺ ($E_0 = -0.41$ V).

In order to estimate an upper limit for the reduction potential using the Nernst equation we have to know the actual concentration of our reductant. This can be done with the aid of our previous tests, where we reduced Eu³⁺ to the Eu²⁺ state ($E_0 = -0.35$ V). This results in a ≥ 0.005 M Cr²⁺ solution. Since zero observed events of Lr are compatible with 3 events at a 95 percent confidence level for Poisson statistics we obtain

an upper limit for the reduction potential of $E_0 \leq -0.44$ V for the Lr³⁺/Lr¹⁺ half reaction. Further searches for Lr¹⁺ in aqueous solutions should be based on electrochemical methods.

1. R.Silva et al. Nucl.Chem Letters, 6, 733 (1970)
2. L.J.Brewer J.Opt.Sci.Am. 61, 1101 (1971)
3. J.P.Desclaux et al. J.Physique 41, 943 (1980)
4. W.Brüchele et al. GSI Scientific Report 83, GSI 84-1 (1984) p.247
5. E.K.Hulet et al., Science 158, 186 (1967)

Figure: α -particle spectra of the trivalent actinides (1) containing 13 events of ²⁶⁰Lr at ≈ 8.0 MeV. Spectrum (2) represents the reduced actinides, i.e. Md²⁺.



Search for Lawrencium as a p-element using on-line isothermal gasphase chemistry

D.T. Jost, H. Gäggeler

EIR Wuerenlingen, CH

B. Eichler

ZfK Rossendorf, DDR

K. Gregorich, D.C. Hoffman, D. Lee, H. Hall, R. Chasteler, R. Henderson

LBL Berkeley, CA

M. Schädel

GSI Darmstadt

Recent calculations including relativistic effects of the ground state configuration of Lr suggest it to be $5f^{14} 7s^2 7p^1$ instead of $5f^{14} 7s^2 6d^1$ as it would be expected from the systematics of the periodic table¹.

Depending on the ground state configuration Lr should chemically behave as an actinide element ($6d^1$) or similar to thallium ($6p^1$). Experimentally actinide elements and p-elements can be separated by a gasphase chemistry technique similar to that developed in the search for super-heavy elements². In this work a quartz chromatography tube with a graphite plug and an inert gas/hydrogen mixture was found to be the most favorable condition to volatilize p-elements and to retain actinides.

Another possibility to separate Lr(p) from actinide elements is the gas chromatography in metal columns. Model calculations by Eichler et al. predict adsorption enthalpies of actinides on various metals³. For Lr the enthalpies are given for the p- and the d-configurations as 187 kJ/mol and 749 kJ/mol⁴ for the adsorption on platinum (best choice for Lr(p)). Other actinides all have adsorption enthalpies above 400 kJ/mol on platinum. An adsorption enthalpy of 187 kJ/mol at a column temperature of 1300 K gives short retention times (seconds) whereas 400 kJ/mol corresponds to a very high retention time of $> 10^5$ min.

The following experiments were performed: A $800 \mu\text{g}/\text{cm}^2$ Bk-249-target was irradiated at the Lawrence Berkeley Laboratory 88"-Cyclotron with a 100 MeV 0-18 beam in order to produce Lr-260 in an $(\alpha,3n)$ reaction. The reaction products were transported with a KCl-gasjet (Carrier gas: He + 4% hydrogen) to an isothermal gaschromatography apparatus, see Figure 1. In the first set of experiments a quartz tube with a graphite plug was kept at 1370 K. In the second set a platinum tube with a graphite plug was used. Elements volatile under these conditions migrated out of the chromatography tube into a gas chamber where they were attached to new KCl aerosols from a second gas-jet (reclustering). This secondary jet was fed into the MG-system where the aerosols carrying the activity were deposited on thin plastic foils mounted on a rotating wheel to assay alpha- and sf-events of the volatile species.

Samples were collected for two minutes and subsequently counted by 6 pairs of surface barrier detectors for 2 minutes each. The energy of all events was registered together with a time mark. Off-line processing was used to evaluate the data.

Preliminary analysis of the data allows at the moment to draw the following conclusions: In the quartz/graphite experiment alpha-activities from Po-211m and Bi-211 were identified on the MG-wheel (p-elements from the 6th period). In the platinum/graphite experiment no activity was observed on the MG-wheel. In both experiments no activity attributable to actinides was found. These experiment therefore did not give any evidence for Lr as a volatile p-element. A further detailed analysis of the experimental data, and possibly further experiments, are needed for a final and conclusive answer to the question of the ground state atomic configuration of Lr.

1. D.L. Keller, Radiochimica Acta, 37, 169 (1984)
2. W. Brüchele et al., J. Less-Common Metals, 122, 425 (1986).
3. B. Eichler et al. Report ZfK-560, Rossendorf (1985).
4. B. Eichler et al., to be submitted to Radiochimica Acta

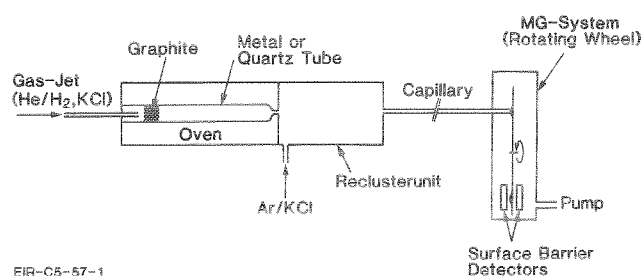


Fig.1: Schematic drawing of the set-up used to search for Lawrencium as a $(7s^2 7p^1)$ -element in the gas-phase.